Coexistence of a self-induced-transparency soliton and a nonlinear Schrödinger soliton in an erbium-doped fiber

Masataka Nakazawa,* Eiichi Yamada, and Hirokazu Kubota
Lightwave Communication Laboratory, NTT Transmission Systems Laboratories, Tokai, Ibaraki-Ken 319-11, Japan
(Received 19 February 1991; revised manuscript received 18 July 1991)

The possibility of observing a self-induced transparency (SIT) in an erbium-doped optical fiber is investigated. A general equation that includes the SIT, the group-velocity dispersion (GVD) of the fiber, and the nonlinear refractive index is discussed. It is shown that for one particular value of waveguide parameters the nonlinear index can balance the GVD, that is, the nonlinear Schrödinger equation (NLS), while maintaining a SIT soliton. This is called a SIT-NLS soliton. The phase change of the SIT-NLS soliton is governed solely by the NLS component, and the pulse delay due to resonance is determined solely by the SIT component when the detuning is zero. Practical parameters for silica-based fibers do not allow the coexistence of a mixed soliton state. A simple derivation of a condition for a SIT-NLS soliton is also presented. The SIT-NLS soliton is computer-run, and it is shown that a stable $2\pi/N=1$ SIT-NLS soliton exists. However, high-order SIT-NLS solitons always split into multiple $2\pi/N=1$ solitons. The NLS property can be preserved when $Z_{sp} \ll L_{abs}$. Finally, the NLS soliton that interacts coherently with erbium ions is studied, and the coherent pulsation that produces multiple narrow pulses is described.

PACS number(s): 42.50.Qg, 42.65.−k

I. INTRODUCTION

Erbium-doped fiber amplifiers (EDFA's) are of great interest since they offer a great potential for opening new fields in optical communications [1–3]. Their typical advantages are a polarization-insensitive high gain of more than 40 dB in the 1.5-μm region, low noise, wide band width, and high output power. Among these excellent characteristics, the wide-band property of greater than 30 nm is very useful for amplifying ultrashort pulses including optical solitons [4–6]. We have recently reported femtosecond optical soliton amplification and trapping in an EDFA [7,8].

The development of these EDFA's offers the possibility for a variety of different fiber applications. When an electric field is guided by the fiber waveguide structure, diffraction effects are eliminated, and this makes it possible for the field to interact with the fiber medium, which has resonance effects over long distances. For example, experiments on self-induced-transparency (SIT) solitons have been reported by many authors [9–12]. However, all of them had to cope in one way or another with diffraction effects that were made even more complicated by nonlinear interactions. Thus, from a purely scientific point of view, it would be beneficial to perform a SIT experiment in an environment in which diffraction effects can be completely ignored. As a related phenomenon, photon echoes of Nd^{3+} ions in optical fibers were observed at low temperatures [13,14].

More importantly, the SIT offers a possibility of pulse shaping and standardization that is different from the nonlinear Schrödinger (NLS) soliton formation [15]. Since some of the energy released in the reshaping of a pulse remains in the medium, and eventually decays via material relaxation processes, pulse shaping by the SIT soliton may yield cleaner pulses than those produced by NLS soliton formation in an essentially loss-free fiber. Recently a SIT digital switch was also proposed [16].

Fundamental work on the SIT-NLS soliton was reported by Maimistov and Manykin in 1983 [17] and more recently related work was reported by Mel'nikov, Nabiev, and Nazarkin [18]. However, the detailed characteristics on SIT-NLS soliton propagation have not yet been clarified.

In the present paper, we present detailed characteristics of SIT-NLS solitons in optical fibers. In Sec. II, SIT equations are briefly reviewed. Then, we introduce the group-velocity dispersion (GVD) and the nonlinear index for NLS solitons in Sec. III. In Sec. IV we show a steady-state SIT-NLS soliton solution. Practical erbium-doped fiber parameters are applied to the SIT-NLS soliton solution in Sec. V, and the possibility of the coexistence of a mixed soliton is investigated. Conditions for obtaining pure SIT solitons ignoring GVD and self-phase-modulation (SPM) are also described. In Sec. VI we discuss the relationship between the soliton period and the absorption length, which characterizes the propagation property of the SIT-NLS soliton. Computer runs for the SIT-NLS soliton are presented in detail in Sec. VII. Finally in Sec. VIII, the propagation of a NLS soliton which interacts coherently with erbium ions is described.

II. THE EQUATIONS OF SIT

In this section we review briefly the equations of a two-level system excited by an E field [19]. In the slow-envelope approximation, the wave equation for the electric-field envelope $E(z,t)$ of a plane wave propagating in the z direction is

 ©1991 The American Physical Society

$$\frac{\partial E}{\partial z}+\frac{1}{v_g}\frac{\partial E}{\partial t}=i\frac{\omega}{2v_g}\frac{P}{\epsilon}\ , \tag{2.1}$$

where v_g is the group velocity of light, ϵ is the dielectric constant, ω is the carrier frequency, and P is the polarization of the medium. The polarization P in a two-level system with amplitudes of wave functions of the upper and lower levels, v_1 and v_2, respectively, is given by

$$P=\langle N_D p_{12}\rho_{21}\rangle = N_D p_{12}\langle v_1 v_2^*\rangle\ , \tag{2.2}$$

where N_D is the particle density, $p_{12}=p_{21}^*$ is the matrix element of the two-level system, ρ_{21} is the density of matrix, and the brackets indicate an average of all inhomogeneously broadened two-level systems. Thus, the equations for the electromagnetic field interacting with the two-level system are

$$\left[\frac{\partial}{\partial z}+\frac{n}{c}\frac{\partial}{\partial t}\right]\left[\frac{p_{21}E}{i\hbar}\right]=\frac{n}{c}\Omega^2\langle v_1 v_2^*\rangle\ , \tag{2.3}$$

where n is the effective index for the linear propagation of the field,

$$\Omega^2=\frac{\omega N_D|p_{12}|^2}{2\hbar\epsilon_0 n^2}\ . \tag{2.4}$$

ϵ_0 is the dielectric constant of free space and ω is the optical carrier frequency. The wave functions v_1 and v_2 obey the differential equations

$$\frac{\partial v_1}{\partial\tau}+i\xi v_1=\tfrac{1}{2}\mathcal{E}v_2\ , \tag{2.5}$$

$$\frac{\partial v_2}{\partial\tau}-i\xi v_2=\tfrac{1}{2}\mathcal{E}^* v_1\ , \tag{2.6}$$

where τ is normalized to Ω and $\mathcal{E}$ is the normalized field

$$\mathcal{E}=\frac{2p_{21}E}{i\hbar\Omega}\ , \tag{2.7}$$

$$\xi=-\frac{\omega-\omega_{21}}{2\Omega}\ , \tag{2.8}$$

and $\hbar\omega_{21}$ is the energy separation of the two center-levels in a homogeneously broadened medium. Coupled equations (2.5) and (2.6) are already the Zakharov-Shabat equations [20]. If one introduces new coordinates

$$\tau=\Omega\left[t-\frac{nz}{c}\right],\qquad \zeta=\frac{\Omega z n}{c}\ , \tag{2.9}$$

(2.5) and (2.6) remain unchanged and (2.3) changes to

$$\frac{\partial\mathcal{E}}{\partial\zeta}=2\langle v_1 v_2^*\rangle\ . \tag{2.10}$$

Equations (2.5), (2.6), and (2.10) are normalized equations for the SIT soliton. They have a simple solution which can be shown by assuming the form

$$\mathcal{E}=4\beta\,\mathrm{sech}2\beta(\tau-\gamma\zeta)\ , \tag{2.11}$$

where β has an arbitrary value, which is the imaginary part of the pole position of the inverse scattering theory and γ is an adjustable parameter related to the time delay due to the SIT effect.

This field partially, or totally, inverts the two-level systems, but returns the population to the ground state, $|v_2|=1$ for $\tau\to\infty$ and $\tau\to-\infty$. The excited level v_1 is zero for both these limits. By substituting (2.11) into Eqs. (2.5) and (2.6), it is shown that the solutions of the equations, v_1 and v_2, are

$$v_2=\sinh[2\beta(\tau-\gamma\zeta)+i\phi]\times\mathrm{sech}2\beta(\tau-\gamma\zeta)e^{i\xi(\tau-\gamma\zeta)} \tag{2.12}$$

and

$$v_1=-\cos\phi\,\mathrm{sech}2\beta(\tau-\gamma\zeta)e^{i\xi(\tau-\gamma\zeta)}\ , \tag{2.13}$$

with

$$\tan\phi=-\xi/\beta\ . \tag{2.14}$$

The derivation of v_1 and v_2 are given in the Appendix. The solutions v_1 and v_2 obey the condition of return to the ground state after passage of the pulse. In addition, we have a condition of

$$|v_1|^2+|v_2|^2=1\ . \tag{2.15}$$

The low level population goes through a phase shift as the pulse "passes through."

Let us consider the average

$$\langle v_1 v_2^*\rangle=\int d\xi\, g(\xi)v_1 v_2^* \tag{2.16}$$

over the distribution of inhomogeneously broadened particles with a symmetric distribution $g(\xi)$, which satisfies $\int d\xi\, g(\xi)=1$. First, it should be noted that groups of particles placed symmetrically around $\xi=0$ give only the real contribution. From Eqs. (2.12) and (2.13), one has

$$v_1 v_2^*=-\frac{\sinh2\beta(\tau-\gamma\zeta)\cos^2\phi}{\cosh^2 2\beta(\tau-\gamma\zeta)}\ . \tag{2.17}$$

Thus, we obtain

$$2\langle v_1 v_2^*\rangle=-2\int d\xi\, g(\xi)\cos^2\phi\,\tanh2\beta(\tau-\gamma\zeta)\times\mathrm{sech}2\beta(\tau-\gamma\zeta)\ . \tag{2.18}$$

The integral on the right-hand side is equal to, or less than, unity. From (2.10), we have

$$2\langle v_1 v_2^*\rangle=\frac{\partial\mathcal{E}}{\partial\xi}=8\beta^2\gamma\,\tanh2\beta(\tau-\gamma\zeta)\mathrm{sech}2\beta(\tau-\gamma\zeta)\ . \tag{2.19}$$

Thus, one obtains

$$8\beta^2\gamma=-2\int d\xi\, g(\xi)\cos^2\phi=-2\int\frac{g(\xi)}{1+(\xi/\beta)^2}d\xi\ . \tag{2.20}$$

When the two-level system is not inhomogeneously broadened, and $g(\xi)$ is a δ function, from (2.20) we find

$$\gamma=\left[\frac{1}{2\beta}\right]^2 . \tag{2.21}$$

The actual space-time dependence of the pulse is

$$\mathcal{E}=4\beta\,\mathrm{sech}2\beta\Omega\left[t-\frac{zn}{c}(1+\gamma)\right], \tag{2.22}$$

where the speed of the pulse is $c/n(1+\gamma)$. The bigger the γ value the slower the pulse. One would expect the greatest slowdown when the medium is not inhomogeneously broadened. Thus, from (2.21) and (2.22) as the pulse becomes shorter, everything else being equal, the slowdown is reduced. This is because the slowdown is due to absorption at the front end of the pulse and gain at the rear. The slope-change accounts for the slowdown, and the speed change is less noticeable as the slope becomes steeper.

It is also noted that the area $\int \mathcal{E}\,d\tau$ of the normalized field is fixed, just as with the soliton solution of the NLS equation. The SIT pulse has a peak field inversely proportional to its temporal width $\tau_s=1/2\beta\Omega$ from (2.22). From (2.7) and (2.11) we have a peak amplitude E_{peak}

$$\begin{aligned}E_{\text{peak}}&=\mathcal{E}_{\text{peak}}\frac{\hbar\Omega}{2|p_{21}|}\\&=4\beta\frac{\hbar\Omega}{2|p_{21}|}\\&=\frac{\hbar}{|p_{21}|\tau_s} .\end{aligned} \tag{2.23}$$

III. ADDITION OF THE GVD AND SPM

SIT works properly only in a plane-wave configuration. The peak field must be such that it returns the population at the line center to the ground state and does likewise for detuned two-level systems. If the product of the field amplitude and the pulse duration does not satisfy this condition, the pulse is not in a stationary steady state. Thus, if we intend to perform guided SIT experiments, the electric field across the SIT medium must be uniform. This requires that the erbium-doped part in the core of the fiber should be thin so that the electric field applied to each erbium ion is constant.

The polarization currents due to the SIT and SPM appear as a sum on the right-hand side of Maxwell's equations. The Maxwell wave equation for an electric field with nonlinear polarizations

$$P_{\text{NL}}(r,z,t)=\tilde{P}_{\text{NL}}(r,z,t)e^{-i(\omega t-kz)} \tag{3.1}$$

is given by

$$\nabla^2 E=\mu_0\sigma\frac{\partial E}{\partial t}+\mu_0\frac{\partial^2 D}{\partial t^2}+\mu_0\frac{\partial^2 P_{\text{NL}}}{\partial t^2} , \tag{3.2}$$

where σ is the conductivity and E is the scalar electric field given by

$$E(r,z,t)=\tilde{E}(z,t)e(r)e^{-i(\omega t-kz)} , \tag{3.3}$$

where $e(r)$ represents the radial field distribution. In (3.1) and (3.3), $\tilde{P}_{\text{NL}}(r,z,t)$ and $\tilde{E}(z,t)$ are slowly varying envelope functions in time and space. With envelope approximations of

$$\frac{\partial^2 P_{\text{NL}}}{\partial t^2}\cong-\omega^2\tilde{P}_{\text{NL}}e^{-i(\omega t-kz)} , \quad (k')^2\ll kk'' ,$$

(3.2) can be rewritten as

$$\begin{aligned}&\{\nabla_T^2 e(r)+[\omega^2\epsilon(r)\mu-k^2]e(r)\}\tilde{E}(z,t)\\&\quad-i2k\left[\frac{\partial}{\partial z}+\frac{\omega\mu_0\sigma}{2k}+k'\frac{\partial}{\partial t}-i\tfrac{1}{2}k''\frac{\partial^2}{\partial t^2}\right]\tilde{E}(z,t)e(r)\\&\quad=-\omega^2\mu\tilde{P}_{\text{NL}}(r,z,t) .\end{aligned} \tag{3.4}$$

Here $k'=1/v_g$ and k was expanded up to the second order in $(\omega-\omega_0)$. Here we are dealing with the propagation mode (single mode) in a fiber waveguide, so $e(r)$ must satisfy

$$\nabla_T^2 e(r)+[\omega^2\epsilon(r)\mu-k^2]e(r)=0 . \tag{3.5}$$

Thus, we have

$$\begin{aligned}&\left[\frac{\partial}{\partial z}+\frac{1}{v_g}\frac{\partial}{\partial t}\right]\tilde{E}(z,t)e(r)\\&\quad=-\frac{\omega\mu}{2k}\tilde{J}_s(r,z,t)+i\tfrac{1}{2}k''\frac{\partial^2\tilde{E}(z,t)}{\partial t^2}e(r)\end{aligned} \tag{3.6}$$

where fiber loss given by $\omega\mu_0\sigma/2k$ was ignored and $\tilde{J}_s$ is now the slow envelope function, in space and time, of the nonlinear polarization density. With the use of the normalization

$$\int|e(r)|^2 dS=1 , \tag{3.7}$$

(3.6) is rewitten as

$$\frac{\partial\tilde{E}}{\partial z}+\frac{1}{v_g}\frac{\partial\tilde{E}}{\partial t}=-\frac{\omega\mu}{2K}\int\tilde{J}_s e^* dS+i\tfrac{1}{2}k''\frac{\partial^2\tilde{E}}{\partial t^2} . \tag{3.8}$$

Now, $\tilde{J}_s$ consists of two parts. One is the SIT contribution, which is represented by

$$\tilde{J}_{s(\text{SIT})}=i\omega\tilde{P}_{\text{SIT}}=i\omega N_D p_{12}\langle v_1 v_2^*\rangle . \tag{3.9}$$

The other is the nonlinear index contribution (SPM), which is given by

$$\begin{aligned}\tilde{J}_{s(\text{NL})}&=i\omega\tilde{P}_{\text{NL}}\\&=i\omega(2nn_2|\tilde{E}|^2)\epsilon_0\tilde{E}\\&=2i\frac{\omega}{c}n_2\sqrt{\epsilon/\mu}|\tilde{E}|^2\tilde{E} .\end{aligned} \tag{3.10}$$

Thus, the total nonlinear polarization is

$$\begin{aligned}-\frac{\omega\mu}{2k}\int\tilde{J}_s e^* dS&=-\tfrac{1}{2}i\omega\sqrt{\mu/\epsilon}N_D p_{12}\langle v_1 v_2^*\rangle\frac{S}{\sqrt{A_{\text{eff}}}}\\&\quad-i\frac{\omega}{c}\frac{n_2}{A_{\text{eff}}}|\tilde{E}|^2\tilde{E} .\end{aligned} \tag{3.11}$$

Here S is the cross section of the SIT core where erbium ions are doped, A_{eff} is the cross section of the mode, and $|e|^2$ is set equal to $1/A_{\text{eff}}$ at its peak. Thus $\int_{\text{SIT}} e^* dS = S/\sqrt{A_{\text{eff}}}$. There are three kinds of radius. One is the fiber core radius of r_a, the second is the spot size (mode-field radius) of w_0,and the third is the SIT core radius of r_s. There is a relationship between them of $r_s < r_a < w_0$, where the fiber core area A_{eff} and S are given by πr_a^2, πw_0^2, and πr_s^2, respectively.

Thus one obtains

$$\frac{\partial \tilde{E}}{\partial z} + \frac{1}{v_g}\frac{\partial \tilde{E}}{\partial t} = -\tfrac{1}{2} i\omega\sqrt{\mu/\epsilon} N_D p_{12} \langle v_1 v_2^* \rangle \frac{S}{\sqrt{A_{\text{eff}}}} - i\frac{\omega}{c}\frac{n_2}{A_{\text{eff}}}|\tilde{E}|^2\tilde{E} + i\tfrac{1}{2}|k''|\frac{\partial^2 \tilde{E}}{\partial t^2} . \quad (3.12)$$

Introducing the transformation of variables

$$t - \frac{z}{v_g} = s ,$$
$$z = z ,$$

we obtain the following final equation as the SIT-NLS equation:

$$(-i)\frac{\partial \tilde{E}}{\partial z} = \tfrac{1}{2}\omega\sqrt{\mu/\epsilon} N_D p_{12} \langle v_1 v_2^* \rangle \frac{S}{\sqrt{A_{\text{eff}}}} + \frac{\omega}{c}\frac{n_2}{A_{\text{eff}}}|\tilde{E}|^2\tilde{E} - \tfrac{1}{2}k''\frac{\partial^2 \tilde{E}}{\partial s^2} . \quad (3.13)$$

Here k'' should be negative for the generation of a NLS soliton.

In order to computer run a SIT-NLS soliton, as described in a later section, (3.13) is further normalized. In addition, Eqs. (2.5) and (2.6) for v_1 and v_2 are also rewritten in the form $F = |v_2|^2 - |v_1|^2 = \rho_{22} - \rho_{11}$ and $M = v_1 v_2^* = \rho_{21}$. This makes it possible to understand intuitively the way in which the dipole phase rotation and the population inversion change with the existence or otherwise of the NLS soliton.

Noting here that $\tau = \Omega s$ and from (2.5)–(2.7), we have

$$\frac{\partial F}{\partial s} = \frac{1}{2}\left[\frac{2p_{21}}{i\hbar}\right](\tilde{E}^* M - \tilde{E} M^*) , \quad (3.14)$$

$$\frac{\partial M}{\partial s} + 2i\xi\Omega M = \left[\frac{2p_{21}}{i\hbar}\right]\tilde{E}F . \quad (3.15)$$

Equations (3.13)–(3.15) are a set of general nonlinear pulse equations for SIT and NLS, in which Eqs. (3.14) and (3.15) are simply the Bloch equations for a two-level atomic system that couples with Eq. (3.13). To normalize the coupled soliton equation, we use the following transformations:

$$\tilde{E} = \frac{\tilde{A}}{(\frac{1}{2}\epsilon_0 cn A_{\text{eff}})^{1/2}} ,$$
$$u = \frac{\tilde{A}}{\sqrt{P_{0(\text{NLS})}}} ,$$
$$x = \frac{s}{\tau_s} , \quad (3.16)$$
$$q = \frac{z}{Z_0} ,$$

where

$$\kappa P_{0(\text{NLS})} = \frac{1}{Z_0} ,$$
$$\kappa = \frac{\omega}{c}\frac{n_2}{A_{\text{eff}}}$$

(nonlinear coefficient),

$$Z_0 = \frac{\tau_s^2}{|k''|}$$

(normalized distance). Thus we obtain

$$\frac{\partial F}{\partial x} = \tfrac{1}{2} i(2W)(uM^* - u^* M) , \quad (3.17)$$

$$\frac{\partial M}{\partial x} + 2i\xi\Omega M = -2iWuF , \quad (3.18)$$

$$(-i)\frac{\partial u}{\partial q} = \frac{Z_0}{\sqrt{P_{0(\text{NLS})}}}\frac{1}{2}\omega N_D p_{12}\left[\frac{A_{\text{eff}}}{2\epsilon_0 cn}\right]^{1/2}\langle M \rangle + \frac{1}{2}\frac{\partial^2 u}{\partial x^2} + |u|^2 u , \quad (3.19)$$

where we put $S = A_{\text{eff}}$. W satisfies

$$P_{0(\text{NLS})} = W^2 \tfrac{1}{2}\epsilon_0 cn\left[\frac{\hbar}{p_{21}\tau_s}\right]^2 A_{\text{eff}} . \quad (3.20)$$

Since $\frac{1}{2}\epsilon_0 cn(\hbar/p_{21}\tau_s)^2 A_{\text{eff}}$ is equal to $P_{0(\text{SIT})}$ using (2.22),

$$W^2 = \frac{P_{0(\text{NLS})}}{P_{0(\text{SIT})}} . \quad (3.21)$$

It should be noted that $2u$ satisfies 2π pulses when $P_{0(\text{NLS})} = P_{0(\text{SIT})}$, that is

$$\tfrac{1}{2}\epsilon_0 cn\left[\frac{\hbar}{p_{21}\tau_s}\right]^2 A_{\text{eff}} = \frac{1}{\kappa Z_0} = \tfrac{1}{2}\epsilon_0 cn\frac{c|k''|}{\omega n_2 \tau_s^2} A_{\text{eff}} .$$

Therefore

$$n_2 = \frac{c|p_{21}|^2|k''|}{\omega\hbar^2}$$

or (3.22)

$$|k''| = \frac{n_2\omega\hbar^2}{c|p_{21}|^2} = \frac{n_2 h^2}{2\pi\lambda|p_{21}|^2} .$$

When this condition is met, there is a secant hyperbolic pulse solution for a SIT-NLS soliton. These results mean

that when W is equal to unity, that is $P_{0(\mathrm{NLS})}=P_{0(\mathrm{SIT})}$, $2u$ in (3.17) and (3.18) and the SIT part of (3.19) completely describe SIT and u also satisfies the NLS soliton part (3.19). It is easily confirmed that (3.22) is the same as

$$\kappa P_{0(\mathrm{NLS})}=\frac{1}{Z_0} ,$$

since

$$\frac{|k''|}{\tau_s^2}=\frac{\omega}{c}\left[\frac{n_2}{\frac{1}{2}\epsilon_0 cn A_{\mathrm{eff}}}\right]P_{0(\mathrm{SIT})} =\kappa P_{0(\mathrm{SIT})} .$$

In the next section, the pulse delay and phase change for the SIT-NLS soliton are described.

IV. STEADY-STATE SOLUTION FOR THE SIT-NLS SYSTEM

As for the SIT soliton, the phase rotation $\phi(q)$ in the z direction can be taken as an arbitrary value. That is, it is possible to replace M with $Me^{i\phi(q)}$. This transformation is useful for understanding how the phase change in the SIT soliton is affected by the NLS soliton

$$\frac{\partial F}{\partial x}=i(uM^*e^{-i\phi(q)}-u^*Me^{i\phi(q)}) , \tag{4.1}$$

$$\frac{\partial(Me^{i\phi(q)})}{\partial x}+2i\xi\Omega Me^{i\phi(q)}=-2iuF , \tag{4.2}$$

$$(-i)\frac{\partial u}{\partial q}=\frac{Z_0}{\sqrt{P_{0(\mathrm{NLS})}}}\tfrac{1}{2}\omega N_D p_{12}\left[\frac{A_{\mathrm{eff}}}{2\epsilon_0 cn}\right]^{1/2}\langle M\rangle e^{i\phi(q)} +\frac{1}{2}\frac{\partial^2 u}{\partial x^2}+|u|^2u . \tag{4.3}$$

Both the SIT and the NLS equations give rise to a hyperbolic secant pulse solution. Therefore, it is expected that a system can be constructed that has these kinds of solutions. Hence, we assume here a normalized solution of the form

$$u=2\eta\,\mathrm{sech}2\eta(x-\delta q)e^{i\alpha q} . \tag{4.4}$$

When we introduce this solution into (4.3), we obtain terms for the forms $\mathrm{sech}(x)$, $\mathrm{sech}^3(x)$, and $\tanh(x)\mathrm{sech}(x)$. That is,

$$\frac{\partial u}{\partial q}=[2\eta\delta\tanh2\eta(x-\delta q)\mathrm{sech}2\eta(x-\delta q) +i\alpha\,\mathrm{sech}2\eta(x-\delta q)]2\eta e^{i\alpha q} ,$$

$$|u|^2u=(2\eta)^3\mathrm{sech}^3 2\eta(x-\delta q)e^{i\alpha q} ,$$

$$\frac{1}{2}\frac{\partial^2 u}{\partial x^2}=[\tfrac{1}{2}(2\eta)^3\mathrm{sech}2\eta(x-\delta q) +(2\eta)^3\mathrm{sech}^3 2\eta(x-\delta q)]e^{i\alpha q} .$$

Setting the coefficients of these terms to equal zero, we obtain the following.

(a) The $\mathrm{sech}(x)$ term:

$$\alpha=\tfrac{1}{2}(2\eta)^2 . \tag{4.5}$$

Thus, the phase change is given by $\alpha q=\frac{1}{2}(2\eta)^2 q$. This means that the phase factor is determined only by the NLS part.

(b) The $\mathrm{sech}^3(x)$ term:

$$(2\eta)^3=(2\eta)^3 .$$

(c) The $\tanh(x)\mathrm{sech}(x)$ term in the case of homogeneous broadening: Since $-\int d\xi\, g(\xi)\cos^2\phi=1$, $2\eta(x-\delta q)$ is equal to $2\beta(\tau-\gamma\zeta)$. Thus, we have

$$(2\eta)^2\delta e^{i\alpha q}=i\frac{Z_0}{\sqrt{P_{0(\mathrm{NLS})}}}\frac{1}{2}\omega N_D p_{12}\left[\frac{A_{\mathrm{eff}}}{2\epsilon_0 cn}\right]^{1/2}e^{i\phi(q)} .$$

In the above equation, the phase terms should be equal, so that

$$\phi(q)=-\frac{\pi}{2}+\alpha q . \tag{4.6}$$

It is important to note that the phase difference at $q=0$ between the dipole and the input field is $\pi/2$, which is the inherent nature of the dipole transition. Furthermore, the z dependence of the phase of the dipole is determined solely by the nonlinear phase change due to the NLS soliton. Also, one has

$$(2\eta)^2\delta=\frac{Z_0}{\sqrt{P_{0(\mathrm{NLS})}}}\frac{1}{2}\omega N_D p_{12}\left[\frac{A_{\mathrm{eff}}}{2\epsilon_0 cn}\right]^{1/2} , \tag{4.7}$$

which determines the pulse delay due to the SIT effect. This means that there is no additional delay contribution from the NLS part when a detuning from the resonance is zero.

Thus, $u=2\eta\,\mathrm{sech}2\eta(x-\delta q)e^{i\alpha q}$ satisfies

$$(-i)\frac{\partial u}{\partial q}=(2\eta)^2\delta\exp\left[i\left[-\frac{\pi}{2}+\tfrac{1}{2}(2\eta)^2 q\right]\right]\langle M\rangle +\frac{1}{2}\frac{\partial^2 u}{\partial x^2}+|u|^2u . \tag{4.8}$$

$1/\delta$ is the normalized speed of the SIT-NLS soliton, but it is determined only by the SIT effect. Let the speed of the SIT-NLS soliton be V. From (2.19) and (2.21)

$$\frac{1}{V}=\frac{n}{c}(1+\gamma) =\frac{n}{c}\left[1-\Omega^2\int_{-\infty}^{\infty}\frac{g(\xi)}{(2\beta\Omega)^2+(2\Omega\xi)^2}d\xi\right] =\frac{n}{c}+\frac{\alpha_{\mathrm{abs}}\tau_s^2}{2\pi g(0)}\int_{-\infty}^{\infty}\frac{g(\Delta\omega)}{1+(\Delta\omega\tau_s)^2}d(\Delta\omega) , \tag{4.9}$$

where $-2\Omega\xi=\omega-\omega_{21}=\Delta\omega$, α_{abs} is the absorption coefficient

$$\alpha_{\mathrm{abs}}=\frac{\pi\omega N_D|p_{21}|^2 g(0)}{\hbar\epsilon_0 cn} , \tag{4.10}$$

and $\pi g(0)=1/\pi\Delta\nu_{\mathrm{FWHM}}$, where FWHM is full width at half maximum. We assume that $g(\Delta\omega)$ is a symmetric function. For the case $2\pi\Delta\nu_{\mathrm{FWHM}}\tau_s\ll 1$,

$$\frac{1}{V}=\frac{n}{c}(1+\Omega^2\tau_s^2) \tag{4.11}$$

and the pulse delay per unit length, $\Delta\tau_D$, is

$$\Delta\tau_D=\frac{1}{V}-\frac{n}{c}=\frac{n}{c}(\Omega\tau_s)^2=\frac{\alpha_{\rm abs}\Delta\omega_{\rm FWHM}\tau_s^2}{4} . \tag{4.12}$$

If $2\pi\Delta\nu_{\rm FWHM}\tau_s$ is much larger than unity,

$$\frac{1}{V}=\frac{n}{c}+\frac{1}{2}\alpha_{\rm abs}\tau_s \tag{4.13}$$

and, therefore, the pulse delay per unit length is given by

$$\Delta\tau_D=\frac{1}{V}-\frac{n}{c}=\frac{1}{2}\alpha_{\rm abs}\tau_s . \tag{4.14}$$

Then we investigate a condition where the GVD and SPM are both negligible. Here, the slowdown due to the SIT, as given by (4.7), must be large compared with the pulse spreading due to the GVD. Since SIT accepts any pulse width as long as the pulse duration is shorter than T_2, this reduces essentially to a pulse-width criterion. This will be described in Sec. VI.

V. POSSIBILITY OF A SIT-NLS SOLITON IN A SILICA-BASED ERBIUM-DOPED FIBER

Using typical values for n_2 and $|p_{12}|$ in silica-based erbium-doped optical fibers, we can investigate whether the SIT-NLS soliton can actually exist in those fibers. The absorption cross section σ at the line center is given by

$$\sigma=\frac{\omega|p_{21}|^2}{\pi\epsilon_0\hbar nc\Delta\nu_H} , \tag{5.1}$$

where $\Delta\nu_H$ is the half width at half maximum (HWHM) of the absorption, $\omega=2\pi\nu$ is the resonance frequency, and h is the Plank constant. Assuming a typical linewidth $\Delta\lambda_H$ of 3 nm ($\Delta\nu_H=\Delta\lambda_H c/\lambda^2$) and $\sigma=5\times10^{-25}$ m^2 [21], one obtains

$$|p_{21}|=1.4\times10^{-32}\ \text{C m}$$
$$=4.7\times10^{-3}\ \text{D} ,$$

where $\lambda=1.55$ μm, $\epsilon_0=8.85\times10^{-12}$ F/m, and $h=6.63\times10^{-34}$ J s. In silica fibers, $n_2=1.2\times10^{-22}$ m^2/V^2. Putting these values into (3.22), $|k''_{\rm SIT\text{-}NLS}|$ which is required for maintaining a hyperbolic secant solution, is

$$|k''_{\rm SIT\text{-}NLS}|=2.7\times10^7\ \text{ps}^2/\text{km} .$$

The negative GVD value at 1.55 μm of a 1.3-μm zero-dispersion single-mode fiber is about -20 ps/km/nm, resulting in

$$|k''_{\rm silica}|=25\ \text{ps}^2/\text{km} .$$

Therefore $|k''_{\rm SIT\text{-}NLS}|$ is six orders of magnitude larger than that of a typical silica fiber. Since the zero dispersion of silica-based fibers cannot be shifted to a wavelength region shorter than around 1.27 μm (the material dispersion dominates), it is very difficult to increase $|k''_{\rm silica}|$ very much. Hence it can be concluded that it is not possible for NLS and SIT solitons to coexist in silica-based erbium-doped fiber.

We estimate here how much peak power is required in order to observe a pure SIT soliton. The peak intensity of a 2π pulse, $I_{\rm peak(SIT)}$, is given by

$$I_{\rm peak(SIT)}=\tfrac{1}{2}cn\epsilon_0(1.76)^2\left[\frac{\hbar}{|p_{21}|\tau_F}\right]^2\ \text{W/m}^2 , \tag{5.2}$$

where $\tau_F(=1.76\tau_s)$ is the FWHM of a hyperbolic secant SIT pulse. At a room temperature, the homogeneous lifetime T_2 is approximately shorter than a picosecond, so that subpicosecond pulses must be used for the SIT experiment. For example, adopting a value of $\tau_F=0.1$ ps.

$$I_{\rm peak(SIT)}=3.4\times10^{19}\ \text{W/m}^2 .$$

Assuming a core diameter of 10 μm for a typical single-mode fiber, the peak power in the fiber $P_{\rm SIT}$ is as large as

$$P_{\rm SIT}=2.7\ \text{GW} .$$

For reference, let us calculate $N=1$ NLS soliton power, $P_{N=1(\rm NLS)}$, given by

$$P_{N=1(\rm NLS)}=0.776\frac{\lambda^3}{(\pi^2cn_2)}\frac{|D|}{\tau_F^2}A_{\rm eff} , \tag{5.3}$$

where $|D|$ is the GVD ($=2\pi c|k''|/\lambda^2$). For $\tau_F=0.1$ ps, $A_{\rm eff}=\pi$ $(5\times10^{-6})^2$ m^2, $\lambda=1.55$ μm, and $|D|=20$ ps/km/nm,

$$P_{N=1(\rm NLS)}=4.8\times10^3\ \text{W} .$$

This result implies that the SIT soliton requires approximately a value six orders of magnitude larger than the NLS soliton, which is consistent with the difference between $|k''_{\rm SIT\text{-}NLS}|$ and $|k''_{\rm silica}|$ as described earlier.

In fact we can derive (4.6) quite easily by using (5.2) and (5.3). For a sech SIT-NLS soliton, the peak power of the SIT soliton should be equal to that of the NLS soliton for a given input pulse width. Noting that $0.776=(1.76)^2/4$ and n_2 in (5.3) has a dimension of m^2/W, so that n_2 should be rewritten as $n_2(2/c\epsilon_0 n)$ when one uses a m^2/V^2 unit, we have

$$P_{\rm SIT}=P_{N=1(\rm NLS)} ,$$
$$\left[\frac{\hbar}{|p_{21}|}\right]^2=\frac{2\pi\lambda|k''|}{4\pi^2n_2} . \tag{5.4}$$

Thus

$$|k''|=\frac{n_2h^2}{2\pi\lambda|p_{21}|^2} . \tag{5.5}$$

In order to observe the SIT solitons in fibers, τ_s should be long enough to decrease the coupled peak power, but it should also be shorter than T_2. This means that the erbium-doped fiber should be cooled down to 4.2 K to prolong the T_2 value. For example, T_2 of Nd^{3+} ions at 4.2 K in an optical fiber is of the order of ~10 ns [13]. For $\tau_F=500$ ps, $P_{\rm SIT}$ is calculated to be

$$P_{\mathrm{SIT}}=107\ \mathrm{W}\ .$$

This power level can be realized by using conventional lasers or optical amplification techniques. A pure SIT soliton will be observable in longer input pulses with a low-temperature erbium fiber.

Similarly, $P_{N=1}$ for $\tau_F=500$ ps is

$$P_{N=1(\mathrm{NLS})}=1.9\times10^{-4}\ \mathrm{W}\ .$$

When we couple the peak power of a 107-W pulse for the SIT measurement, it corresponds to the excitation of a very-high-order NLS soliton. Since the peak power of the N soliton is given by

$$P_N=N^2P_{N=1(\mathrm{NLS})}\ ,$$

N is as large as 751. In order to remove the NLS soliton effect and to observe pure SIT, the GVD should be as small as possible, resulting in a large extension of the soliton period in comparison to the absorption wavelength. Hence, a zero-dispersion fiber at the resonance length is recommended. This will be discussed in detail in the next section.

VI. ABSORPTION LENGTH, SOLITON PERIOD, AND PULSE DELAY

The absorption length L_{abs} is defined by the length over which the transmitted intensity falls to $1/e$ of its original intensity

$$L_{\mathrm{abs}}=1/\alpha_{\mathrm{abs}}\ . \tag{6.1}$$

In erbium-doped fibers, the absorption at 1.535 μm is about 20 dB for a doping concentration of 1000 ppm (0.1 Wt %). Hence, $L_{\mathrm{abs}}=(10\log_{10}e)/20=0.21$ m. For a 1-ppm concentration, the absorption is about 2.4×10^{-3} dB/km, L_{abs} is 1.8 km.

On the other hand, the soliton period Z_{sp} for the NLS soliton is given by

$$Z_{\mathrm{sp}}=0.322\left[\frac{\pi^2c}{\lambda^2}\right]\frac{\tau_F^2}{|D|}\ . \tag{6.2}$$

For $\tau_F=0.1$ ps, $|D|=20$ ps/km/nm, Z_{sp} becomes 0.2 m, and for $\tau_F=500$ ps, it becomes as large as 5×10^3 km.

From (4.7), δ for a $\eta=\frac{1}{2}$ standard soliton with homogeneous broadening can be rewritten as

$$\begin{aligned}\delta&=\frac{Z_0}{\sqrt{P_{0(\mathrm{NLS})}}}\frac{1}{2}\omega N_D p_{12}\left[\frac{A_{\mathrm{eff}}}{2\epsilon_0 cn}\right]^{1/2}\\&=\Omega^2\tau_F\frac{n}{c}Z_0\\&=\frac{Z_{\mathrm{sp}}}{L_{\mathrm{abs}}}(\Delta\nu_F\tau_s)\ .\end{aligned} \tag{6.3}$$

$\Delta\nu_F\tau_s$ is of the order of unity, and therefore, δ indicates the ratio of the soliton period Z_{sp} to the absorption length L_{abs}. For example, when $Z_{\mathrm{sp}}\gg L_{\mathrm{abs}}$ the SIT effect appears in the early stages of the pulse propagation and is dominant in the SIT-NLS soliton system. By using (4.12) and $|D|=(2\pi c/\lambda^2)|k''|$, $Z_{\mathrm{sp}}\gg L_{\mathrm{abs}}$ can be rewritten as

$$\frac{n}{c}\Omega^2\tau_s^2\gg|D|\Delta\lambda\ .$$

Here from (4.12), $(n/c)\Omega^2\tau_s^2$ is the pulse delay per unit length ($\Delta\tau_D$) due to the SIT effect and $|D|\Delta\lambda$ is the pulse broadening due to the GVD. This indicates that the SIT contribution is much larger than the NLS one. For $Z_{\mathrm{sp}}\cong L_{\mathrm{abs}}$, the SIT and NLS have a strong mutual interaction. For $Z_{\mathrm{sp}}\ll L_{\mathrm{abs}}$ the NLS effects dominate in the system. For a $\eta=\frac{1}{2}$ standard soliton ($\beta=\frac{1}{2}$), $\Omega\tau_s=1$, so that we may write

$$\delta=\frac{Z_0}{(n/c)\tau_s}\ .$$

This indicates that when the normalized distance Z_0 is equal to the propagation distance $[(n/c)\tau_s]$ given by the pulse width, δ becomes unity.

We have learned that the observation of a SIT soliton for a 0.1-ps pulse is very difficult since the peak power in an erbium-doped fiber is in the gigawatt region. Expansion of the pulse width to a few hundred picoseconds to nanoseconds might be useful for a SIT measurement at low temperatures, which would mean that Z_{sp} became quite long. Therefore, in most cases,

$$L_{\mathrm{abs}}\ll Z_{\mathrm{sp}}\ .$$

This means that the SIT phenomenon will be observable in the early stage of the erbium fiber before the occurrence of nonlinear wave-form changes due to the NLS soliton.

Let us estimate the pulse delay τ_D for a fiber length of L(m) and an input pulse with of τ_F. Two-level resonance is inhomogeneously broadened in rare-earth ions in a glass medium. For a Nd^{3+}-doped silica-based fiber, the homogeneous lifetime T_2 at 4.2 K is ~10 ns [12] so that a τ_F of 500 ps is sufficiently short to allow the SIT to be measured. However, we have to take into account the inhomogeneous broadening $\Delta\lambda_{\mathrm{FWHM}}$, which is ~3 nm at 4.2 K at 1.535 μm. Therefore, the homogeneous linewidth is much narrower than the inhomogeneous one, so that from (4.14)

$$\begin{aligned}\tau_D&=\tfrac{1}{2}\alpha_{\mathrm{abs}}L\tau_s\\&=0.284\alpha_{\mathrm{abs}}L\tau_F\ .\end{aligned}$$

The fiber length L must be much longer than the pulse length given by $c\tau_F/n$ in order to observe pure τ_D. For $\alpha_{\mathrm{abs}}=4.6\ \mathrm{m}^{-1}$, which approximately corresponds to a 1000-ppm doping concentration, $\tau_F=500$ ps, $\Delta\lambda_{\mathrm{FWHM}}=3$ nm, an inhomogeneous lifetime $T_2^*=4.4\times10^{-13}$ s, T_2 at 4.2 K $=\sim10$ ns, and $L=2$ m, $\tau_D=1.3$ ns. This can be easily observed with a fast photodetector.

VII. COMPUTER SIMULATION OF SIT-NLS SOLITONS

In this section we use computer runs to show how the SIT-NLS soliton wave-form changes when it propagates

down a fiber. Although it is usually very useful to adopt the beam propagation method (BPM) [22], it cannot be used in the present soliton because there is no explicit u dependence on $\langle M \rangle$ in (4.3). Thus, the Runge-Kutta method was used to calculate the time dependences of ρ_{12} and $\rho_{22}-\rho_{11}$ [(3.17) and (3.18)]. These SIT equations couple with the main equation given in (4.3) through the z dependence. Here for simplicity the coefficient of $\langle M \rangle$ is replaced with δ,

$$(-i)\frac{\partial u}{\partial q}=\delta\langle M\rangle+\frac{1}{2}\frac{\partial^2 u}{\partial x^2}+|u|^2 u \ . \tag{7.1}$$

To computer-run the above partial differential equation, the three-point differential method was used [23]. In addition, $\langle M \rangle$ is replaced with M by assuming a homogeneous broadening, and the frequency detuning from the resonance is set to be zero, i.e., $\xi=0$.

The initial conditions are $\rho_{22}(t=0)=0$, $\rho_{11}(t=0)=1$, $\rho_{12}(t=0)=0$, and $u=N\,\mathrm{sech}(x)$. The midpoint method was adopted, rather than the conventional Euler method, to increase accuracy in the propagation direction [23]. The accuracy was checked by calculating the degree of energy conservation of the soliton (integration of the 2π pulse intensity) after a long propagation. In addition, the stepsize Δz for SIT-NLS solitons was decreased to 1/100 that of Δz for the SIT to maintain the stability of the present method.

Before we investigate the detailed characteristics of the SIT-NLS solitons, we show the importance of (3.22) to the realization of the stable mixed soliton state. As given in (3.20) and (3.21), if W is not equal to unity, in other words if 2π SIT does not correspond to the $N=1$ NLS soliton, a stable SIT-NLS soliton cannot exist. That is, an arbitrary u is acceptable for (3.19) since there is no explicit expression of u for M. However, from the viewpoint of the SIT soliton propagation, $W=1$ is the only acceptable condition for (3.17) and (3.18) to maintain 2π pulses.

When W is equal to 2, i.e., $\pi/N=1$, the pulse eventually disperses and a stable pulse cannot propagate. This is shown in Fig. 1(a), where the delay δ is equal to unity. Figure 1(b) shows $2\pi/N=2$ pulses, which are also found to be unstable.

The propagation of stable SIT-NLS solitons is shown in Figs. 2–7. Waveforms (a) and (b) in each figure correspond to the SIT soliton and the SIT-NLS soliton, respectively. With this, we can compare the differences between the SIT-NLS soliton and the SIT or NLS solitons. Figure 2(a) is a wave-form change for a 2π SIT soliton with $\delta=1$. With the addition of the NLS part as seen in Fig. 2(b), a stable $2\pi/N=1$ SIT-NLS soliton propagates. The delay for a $2\pi/N=1$ SIT-NLS soliton is exactly the same as that for a 2π SIT soliton. This agrees with the theory described in Sec. IV. When there is a detuning from the resonance, the NLS term produces an additional delay due to the group velocity of dispersion of the fiber. When δ is changed to 3 as shown in Figs. 3(a) and 3(b), the delay due to the resonance is three times as large as that for $\delta=1$, as we expected. Nevertheless it is important to note that the delay for a 2π SIT soliton with $\delta=3$ is the same as that for a $2\pi/N=1$ SIT-NLS soliton with $\delta=3$.

Wave-form changes for a 4π SIT soliton and a $4\pi/N=2$ SIT-NLS soliton are shown in Figs. 4 and 5, where δ is 1 and 3, respectively. As seen in these figures, the $4\pi/N=2$ soliton eventually splits into two 2π solitons, even in the presence of the NLS component. The SIT-NLS soliton cannot preserve the NLS soliton property. If we look closely at transient wave-form changes during the first Z_0, a wave-form change caused by the addition of the NLS component can be found. However, this does not influence the pulse delay due to the SIT effect. For Fig. 5, the splitting of the soliton into 2π pulses occurs faster than that in Fig. 4, since δ is 3. Under this condition, the absorption length for the SIT is shorter than the soliton period for the NLS.

Wave-form changes for the 6π SIT and $6\pi/N=3$ SIT-NLS solitons are shown in Figs. 6 and 7, where (a) is SIT solitons and (b) is $6\pi/N=3$ solitons. It is important to note that the delay for the $6\pi/N=3$ SIT-NLS soliton is exactly the same as that for the 6π SIT soliton, although the wave-form change, mainly caused by the nonlinear wave-form change due to the NLS component, between

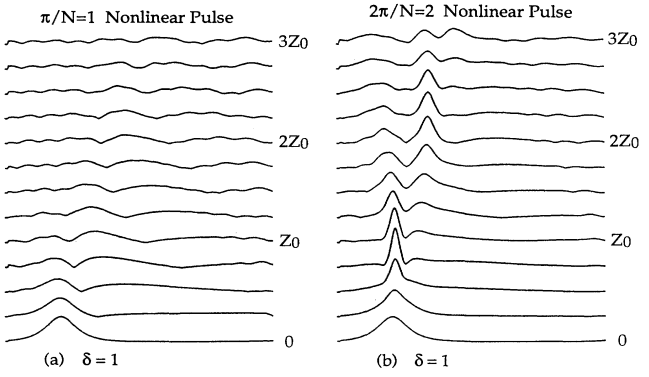

FIG. 1. Unstable propagation of $\pi/N=1$ and $2\pi/N=2$ nonlinear pulses. The stable SIT-NLS soliton pulse cannot propagate since W is not unity.

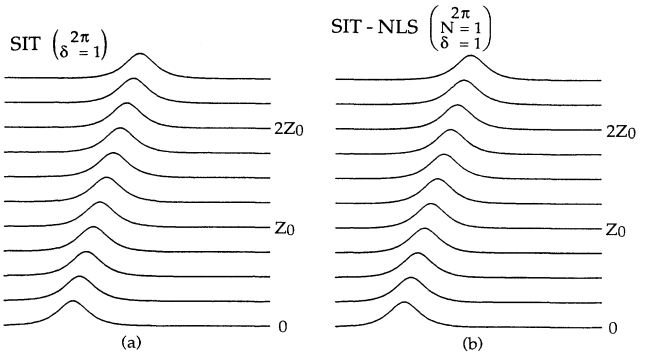

FIG. 2. Stable $2\pi/N=1$ SIT-NLS soliton propagation for $\delta=1$. (a) SIT, (b) SIT-NLS. The pulse delay is attributed to the resonance and the delay in (a) is the same as that in (b).

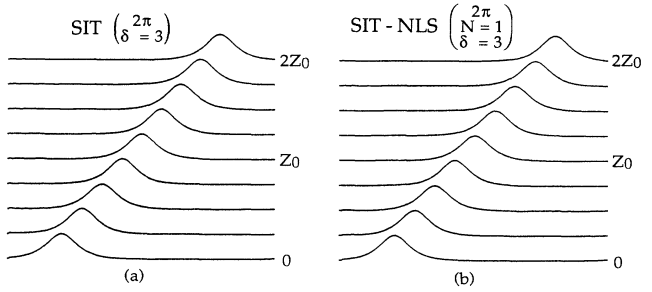

FIG. 3. Stable $2\pi/N=1$ SIT-NLS soliton propagation for $\delta=3$. (a) SIT (2π), (b) SIT-NLS. The pulse delay is three times larger than that in Fig. 2.

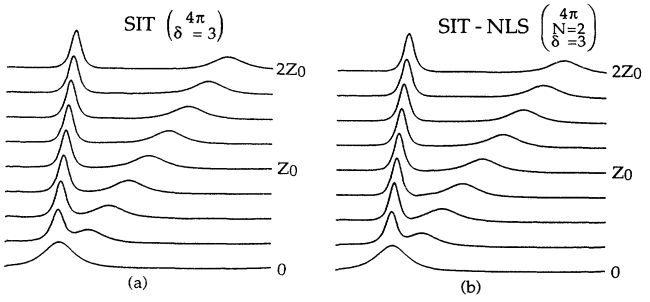

FIG. 5. $4\pi/N=2$ SIT-NLS soliton for $\delta=3$. (a) SIT (4π), (b) SIT-NLS. The delay is three times larger than that of Fig. 4.

$z=0$ and $z=2Z_0$ is quite different from that for the SIT only. It is also clearly seen that the pulse-splitting speed of the $\delta=3$ SIT-NLS soliton is faster than that of the $\delta=1$ SIT-NLS soliton. For example, compare the wave-form changes at $z=2Z_0$ in Figs. 6 and 7.

Changes in the population difference $\rho_{22}-\rho_{11}$ for 2π, 4π, and 6π SIT solitons and for $2\pi/N=1$, $4\pi/N=2$, and $6\pi/N=3$ SIT-NLS solitons are shown in Fig. 8, where δ is equal to unity. (a1), (a2), and (a3) correspond to 2π, 4π, and 6π SIT solitons and (b1), (b2), and (b3) correspond to $2\pi/N=1$, $4\pi/N=2$, and $6\pi/N=3$ SIT-NLS solitons, respectively. For the 2π SIT and $2\pi/N=1$ SIT-NLS solitons, the population is changed from -1 to 1 by the π pulse and it is returned to -1 by the remaining π-pulse component. For 4π the SIT and $4\pi/N=2$ SIT-NLS solitons, the population changes twice between -1 and 1. Similarly, for the 6π SIT and $6\pi/N=3$ solitons, three 2π pulse changes in $\rho_{22}-\rho_{11}$ are excited at the input end. Note here that an asymmetric population change is seen at $z=2.5Z_0$ in Fig. 8(b3), although there is no great difference between Figs. 6(a) and 6(b) at $z=2.5Z_0$. This population change is caused by the nonlinear phase change caused by the NLS component.

We investigate here $|\rho_{21}|^2$ and the phase of ρ_{21} in Figs. 9–11, corresponding to the 2π SIT and $2\pi/N=1$ SIT-NLS solitons, the 4π SIT and $4\pi/N=2$ SIT-NLS solitons, and the 6π SIT and $6\pi/N=3$ SIT-NLS solitons, respectively. There is a $\pi/2$ phase change from a peak of the field amplitude in the phase of ρ_{21} for 2π SIT shown in Fig. 9(b), which agrees with our result shown in (4.6). This is the inherent phase difference between the electric field and the phase of the dipole moment. However, it should be noted that there is no phase change due to pulse propagation as shown by the dashed line of Fig. 9(b). Although $|\rho_{21}|^2$ for a $2\pi/N=1$ SIT-NLS soliton is the same as that of 2π SIT, the phase of ρ_{21} is different from 2π SIT. The phase rotation is entirely determined by the nonlinear phase change due to the NLS soliton component. That is,

$$\phi(z)=\tfrac{1}{2}(2\eta)^2\frac{z}{Z_0}$$
$$=1.25 \text{ rad}$$

for $\eta=\frac{1}{2}$ and $z=2.5Z_0$, which agrees well with the present computer result as shown in Fig. 9(d).

In Figs. 10 and 11, $|\rho_{21}|^2$ changes very rapidly between 0 and 1, and the phase of ρ_{21} also changes between $\pi/2$

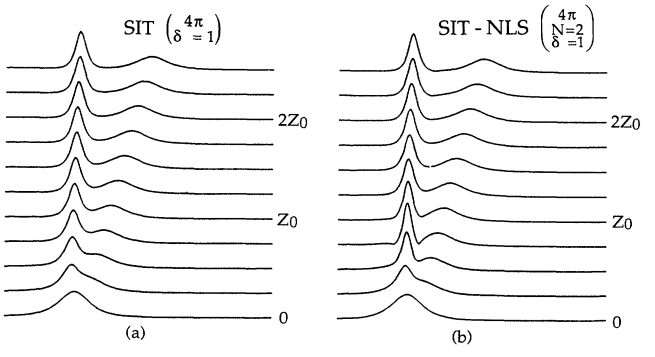

FIG. 4. $4\pi/N=2$ SIT-NLS soliton for $\delta=1$. (a) SIT (4π), (b) SIT-NLS. The SIT-NLS pulse splits into $2\pi/N=1$ SIT-NLS solitons. The delay for SIT is the same as that for SIT-NLS, even when $2\pi/N=2$.

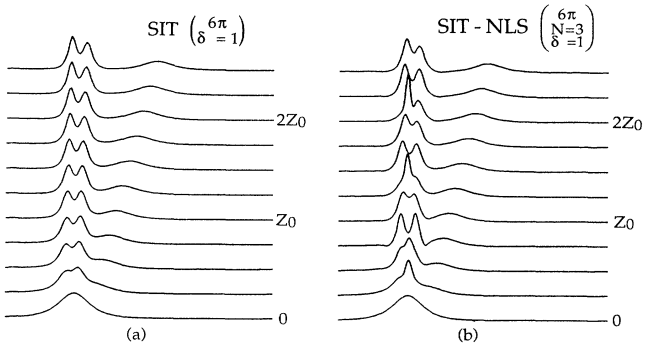

FIG. 6. $6\pi/N=3$ SIT-NLS soliton for $\delta=1$. (a) SIT (6π), (b) SIT-NLS. The wave-form change due to the NLS part is seen clearly in (b), but the delay is the same as that in (a).

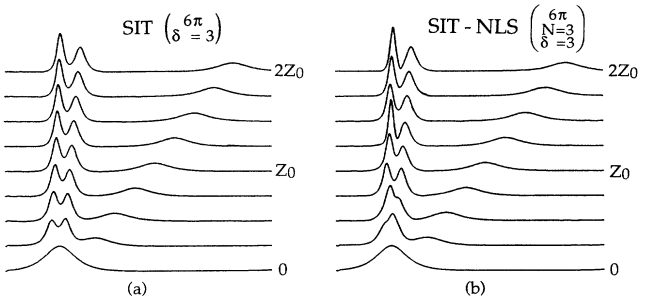

FIG. 7. $6\pi/N=3$ SIT-NLS soliton for $\delta=3$. (a) SIT (6π), (b) SIT-NLS. The pulse splitting is faster than that in Fig. 6.

and $-\pi/2$. In both figures, pulse splitting into 2π pulses is clearly seen. The phase shifts of the split 2π solitons for $4\pi/N=2$ and $6\pi/N=3$ SIT-NLS solitons are also 1.25 rad at $z=2.5Z_0$ [see Figs. 10(d) and 11(d)], which are the same as that of the $2\pi/N=1$ SIT-NLS fundamental soliton. The $6\pi/N=3$ soliton eventually splits into three 2π solitons. Neither can preserve the $N=3$ NLS soliton property.

Figure 12 shows the wave-form change of a $4\pi/N=2$ SIT-NLS soliton for $\delta=0.2$, in which the soliton period is shorter than the absorption length. In one normalized distance from $z=0$ to $z=Z_0$, it is clearly seen that an

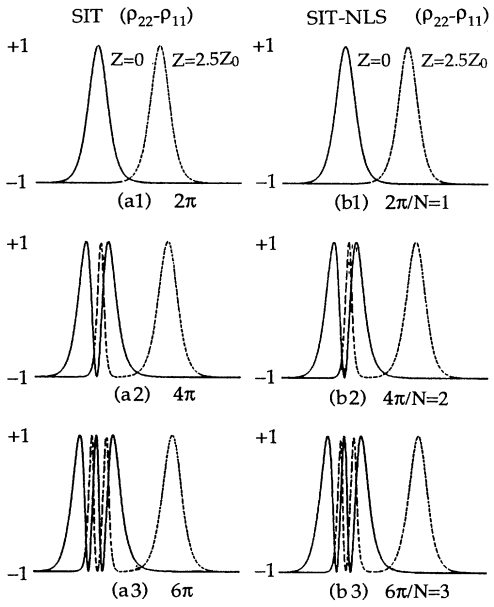

FIG. 8. Changes in the population difference $\rho_{22}-\rho_{11}$ for different input amplitudes. $\delta=1$. Solid lines are at $z=0$ and dashed lines are at $z=2.5Z_0$. (a1), (a2), and (a3) correspond to 2π, 4π, and 6π SIT solitons and (b1), (b2), and (b3) correspond to $2\pi/N=1$, $4\pi/N=2$, and $6\pi/N=3$ SIT-NLS solitons, respectively. $\rho_{22}-\rho_{11}$ changes from -1 to 1 and returns to -1 from 1 every 2π.

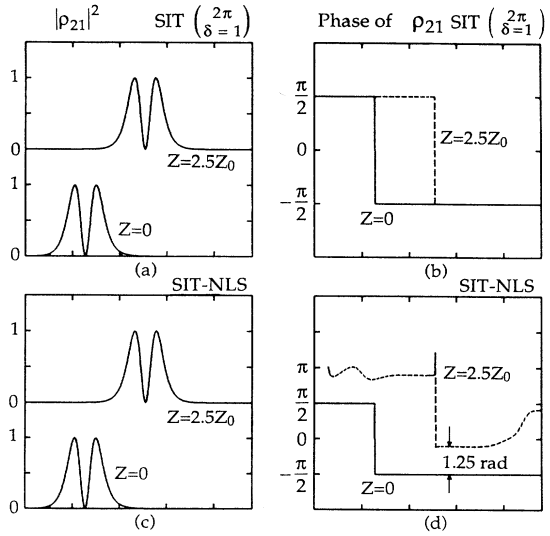

FIG. 9. Comparison of dipole changes for SIT solitons and $2\pi/N=1$ SIT-NLS solitons. $|\rho_{21}|^2$ and the phase of ρ_{21} for 2π SIT are shown in (a) and (b), respectively. Those for the $2\pi/N=1$ SIT-NLS soliton are shown in (c) and (d). There is a nonlinear phase change which arises from the appearance of the NLS part in the SIT-NLS soliton.

$N=2$ NLS soliton is excited, and the hump on the left-hand side of the pulse peak is growing, resulting in pulse splitting due to the SIT component. In this case, $Z_{sp} \ll L_{abs}$, so that the early stage of the pulse propagation is dominated by the wave-form changes due to the $N=2$ NLS soliton property, and eventually the pulse

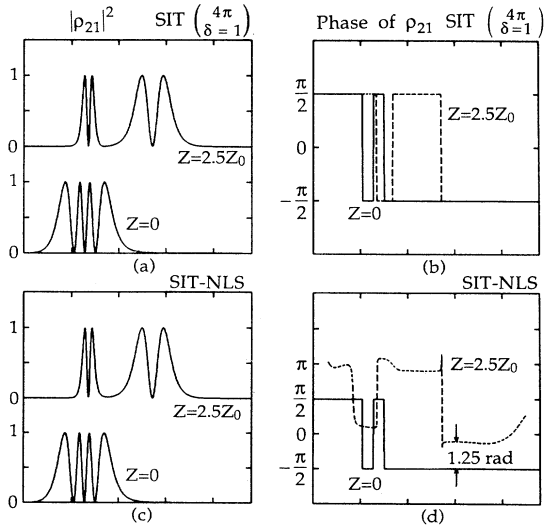

FIG. 10. Comparison of dipole changes for SIT solitons and $4\pi/N=2$ SIT-NLS solitons. $|\rho_{21}|^2$ and the phase of ρ_{21} for 4π SIT are shown in (a) and (b), respectively. Those for $4\pi/N=2$ SIT-NLS solitons are shown in (c) and (d), respectively.

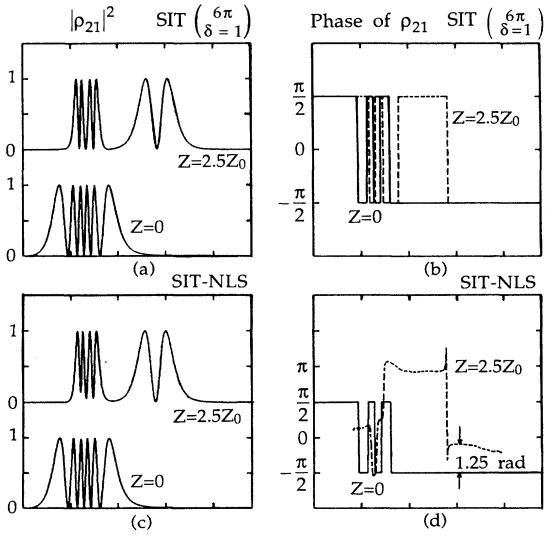

FIG. 11. Comparison of dipole changes for SIT solitons and $6\pi/N=3$ SIT-NLS solitons. $|\rho_{21}|^2$ and the phase of ρ_{21} for 6π SIT are shown in (a) and (b), respectively. Those for $6\pi/N=3$ SIT-NLS solitons are shown in (c) and (d), respectively.

splits into two 2π solitons. To investigate the delay difference between SIT and SIT-NLS solitons, both solitons are propagated over $12.5Z_0$, as shown in Fig. 13. As a result, it is found that the delay is the same as that

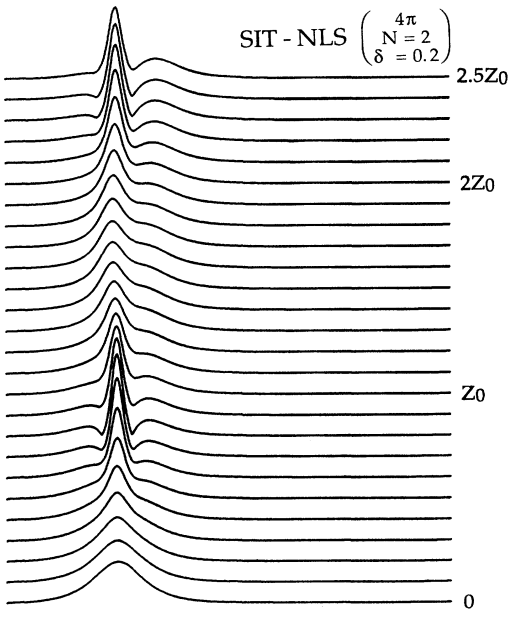

FIG. 12. Interaction between the SIT part and the NLS part in a $4\pi/N=2$ SIT-NLS soliton with $\delta=0.2$. A small δ lengthens the interaction. Here, a wave-form change due to the $N=2$ NLS soliton is clearly seen, accompanying a pulse splitting on the right wing of the main pulse.

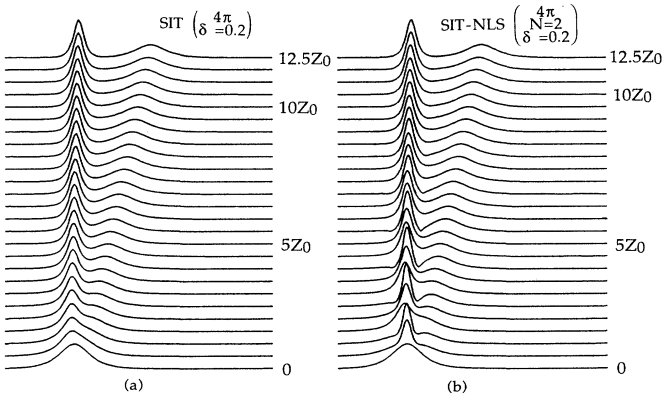

FIG. 13. Comparison between the pulse delays of a 4π SIT soliton and a $4\pi/N=2$ SIT-NLS soliton where $\delta=0.2$. It is noted that the delay for the SIT-NLS soliton is identical to that of the SIT soliton.

of a 2π SIT soliton for $\delta=0.2$. This is surprising since the NLS term has no effect on the delay in the case of zero detuning, even when the SIT-NLS soliton experiences a strong interaction between the SIT and the NLS components over long distances. That is, there is no additional change in the delay in the SIT-NLS soliton, if $W=1$ and high-order perturbation are not applied to the NLS component.

VIII. NLS SOLITON PROPAGATION COHERENTLY INTERACTING WITH A RESONANT TWO-LEVEL SYSTEM

Thus far we have described the SIT-NLS soliton propagation where W in Eq. (3.20) is equal to unity. However, W for a practical erbium fiber with a GVD of -5 ps/km/nm and $|p_{12}|=1.4\times10^{-32}$ C m is much smaller than unity. That is,

$$W=\left[\frac{c|k''||p_{12}|^2}{\omega n_2\hbar^2}\right]^{1/2}$$
$$\cong 4.8\times10^{-4}\ . \tag{8.1}$$

Although the contribution of the two-level coherent interaction to the NLS propagation is small, the interesting feature of coherent pulsation appears. Therefore, this section describes the coherent interaction between NLS solitons and erbium ions.

Introducing time constant T_2 for the dipole relaxation between ${}^4I_{13/2}$ and ${}^4I_{15/2}$ of erbium ions, time constant T_1 of the population inversion, and the soliton self-frequency shift (SSFS) [24,25], Eqs. (3.17)–(3.19) can be rewritten as

$$\frac{\partial F}{\partial x}+\frac{\tau_s}{T_1}F=\tfrac{1}{2}i(2W)(uM^*-u^*M)\ , \tag{8.2}$$

$$\frac{\partial M}{\partial x}+\frac{\tau_s}{T_2}M+2i\xi\Omega M=-2iWuF\ , \tag{8.3}$$

$$(-i)\frac{\partial u}{\partial q}=\frac{Z_0}{\sqrt{P_{0(\mathrm{NLS})}}}\tfrac{1}{2}\omega N_D p_{12}\left[\frac{A_{\mathrm{eff}}}{2\epsilon_0 cn}\right]^{1/2}\langle M\rangle + \frac{1}{2}\frac{\partial^2 u}{\partial x^2}+|u|^2u+\frac{\tau_n}{\tau_s}u\frac{\partial}{\partial x}|u|^2 . \quad (8.4)$$

For a zero-detuning condition of $\xi=0$, $\tau_s \ll T_1$, and $\tau_s \gg T_2$, which means that the input pulse cannot interact coherently with erbium ions, that is a noncoherent condition, one obtains

$$M=-2iWuF\frac{T_2}{\tau_s} , \quad (8.5)$$

$$F=\exp\left[\int_0^x -4W^2\frac{T_2}{\tau_s}|u|^2dx\right] . \quad (8.6)$$

Since $T_2/\tau_s \ll 1$, $M(q,\tau)$ can be expressed as

$$M(q,\tau)\cong -2iW\frac{T_2}{\tau_s}u(q,\tau) . \quad (8.7)$$

From Eqs. (8.4) and (8.7), the following is obtained:

$$\frac{Z_0}{\sqrt{P_{0(\mathrm{NLS})}}}\frac{1}{2}\omega N_D p_{12}\left[\frac{A_{\mathrm{eff}}}{2\epsilon_0 cn}\right]^{1/2}M=i\frac{\omega N_D|p_{12}|^2T_2}{\epsilon_0 cn\hbar}Z_0u ,$$
$$=i\alpha_{\mathrm{abs}}Z_0u$$
$$=i\Gamma_{\mathrm{abs}}u , \quad (8.8)$$

where α_{abs} is given by Eq. (4.10) and Γ_{abs} is the normalized resonant absorption coefficient. Therefore, for the noncoherent condition which can be characterized by the fact that the gain bandwidth is much broader than the spectral width of the input pulse, the following equation can be applied:

$$(-i)\frac{\partial u}{\partial q}=i\Gamma_{\mathrm{abs}}u+\frac{1}{2}\frac{\partial^2 u}{\partial x^2}+|u|^2u+\frac{\tau_n}{\tau_s}u\frac{\partial}{\partial x}|u|^2 . \quad (8.9)$$

When Γ_{abs} is small, adiabatic soliton broadening occurs. When the absorption coefficient is, for example, 20 dB/m for a 1000-ppm fiber, a strong attenuation occurs through the fiber, and only the SIT soliton is transmitted. When Γ_{abs} is positive because of population inversion, adiabatic soliton narrowing or the excitation of high-order solitons occurs.

The number of erbium ions per cm^3 is given as follows. The density of SiO_2 is 2.22 $\mathrm{g/cm}^3$ and the atomic number of erbium ions is 167.26 g/mol. When the weight of erbium ions in 1 cm^3 SiO_2 is 1 ppm (1×10^{-4} wt %), it becomes 2.22×10^{-6} $\mathrm{g/cm}^3$. Thus the number of erbium ions is given by $(2.22\times10^{-6}/167.26)(6.02\times10^{23})=8\times10^{15}/\mathrm{cm}^3$. For example, the number of erbium ions in a 1000-ppm erbium fiber is $8\times10^{18}/\mathrm{cm}^3$. This value can be confirmed in a different way using the absorption cross section given in Eq. (5.1). The σ of erbium ions is 0.5×10^{-20} cm^2. For a 1000-ppm fiber, the absorption is approximately 20 dB/m. Since $N_0\sigma=\alpha_{\mathrm{abs}}$, N_0 is $9.2\times10^{18}/\mathrm{cm}^3$, which agrees well with the above-mentioned result.

Here we analyze a population-inverted case, in which the initial condition is given by $\rho_{22}(0)-\rho_{11}(0)=1$. In this case, both coherent and noncoherent pulse propagation exhibit interesting features. Figure 14(a) shows a coherent NLS soliton propagation for $\tau_s=250$ fs, $T_2=250$ fs, GVD$=-5$ ps/km/nm, and $N=5\times10^{18}/\mathrm{cm}^3$, which corresponds to an erbium-ion doping concentration of 620 ppm. The absorption coefficient is 2.9 m^{-1}. The initial amplitude of the input sech(x) pulse is unity, and the SSFS was not taken into account. As shown in Fig. 14(a), multiple pulses are generated. Although the area of the pulse is not of the order

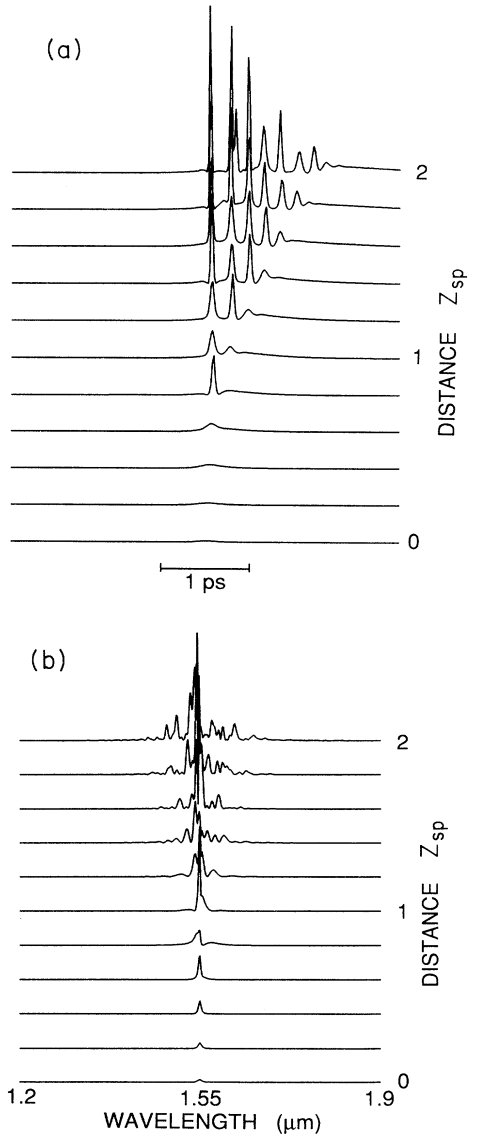

FIG. 14. A NLS soliton which coherently interacts with erbium ions. $\tau_s=250$ fs, $T_2=250$ fs, GVD$=-5$ ps/km/nm, and $N_0=5\times10^{18}/\mathrm{cm}^3$, which corresponds to an erbium-ion doping concentration of 620 ppm. (a) Wave form, (b) spectrum. The input pulse is an $N=1$ soliton and the SSFS is not taken into account. A coherent pulsation occurs due to the interaction with erbium ions.

of π, a coherent pulsation similar to a π pulse in a coherent amplifier occurs. This is a new phenomenon caused by the coherent interaction. The spectrum of the waveform in Fig. 14(a) is shown in Fig. 14(b), in which the sideband corresponding to a repetition rate of the multiple pulses is clearly seen. If the process is noncoherent, ordinary soliton growth from $N=1$ to $N=2$ or 3 NLS soliton is observed. When the SSFS ($\tau_n=5.9\times10^{-15}$ s) is taken into account, the waveforms in Fig. 14(a) change as shown in Fig. 15(a), in which a sharp soliton pulse is delayed by the SSFS. Figure 15(b) shows its spectral change. As shown in Fig. 15(b), the SSFS changes the carrier wavelength of the soliton to longer wavelengths, resulting in a soliton delay. According to Figs. 15(a) and 15(b), it can be said that the generation of multiple pulses (coherent pulsation) is suppressed by the wavelength shift. This is reasonable since the wavelength shift causes a detuning from the resonance.

Changes in the waveform for $T_2=100$ fs, $\tau_s=250$ fs, and no SSFS are shown in Fig. 16(a). The spectrum of the waveform is shown in Fig. 16(b). This condition corresponds to noncoherent amplification of the NLS soliton. A clear NLS soliton evolution from an $N=1$ to $N=2$ soliton can be seen. Since $T_2<\tau_s$, the soliton is gradually amplified, and adiabatic soliton amplification occurs for low gain. However, when the amplified pulse has a narrower width with a higher peak intensity compared to the input pulse because of the soliton narrowing and the excitation of high-order solitons, τ_s becomes

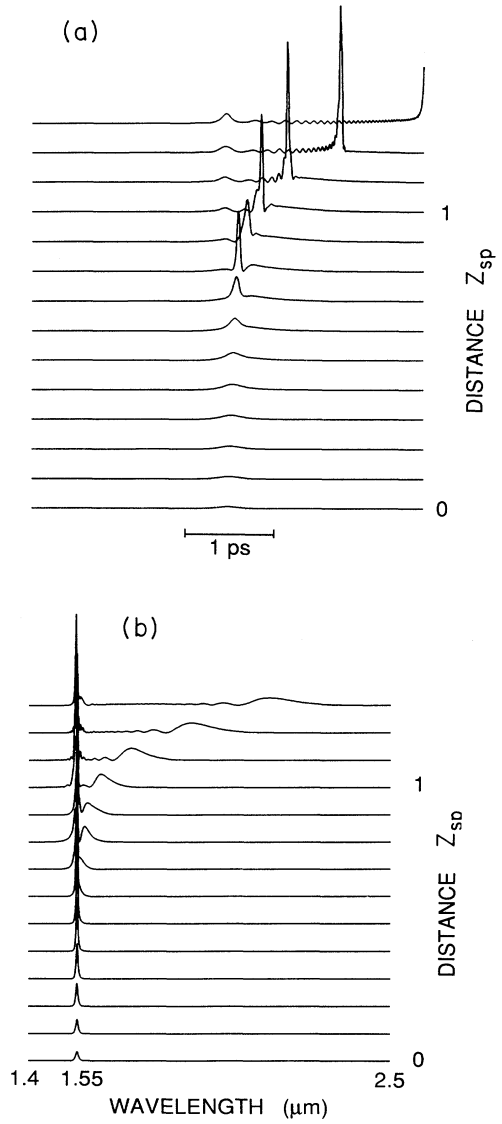

FIG. 15. A NLS soliton with the SSFS which is coherently interacting with erbium ions. $\tau_n=5.9\times10^{-15}$ s and other parameters are the same as those in Fig. 14. (a) Wave form, (b) spectrum. A sharp soliton pulse is generated, which is delayed behind the ripple.

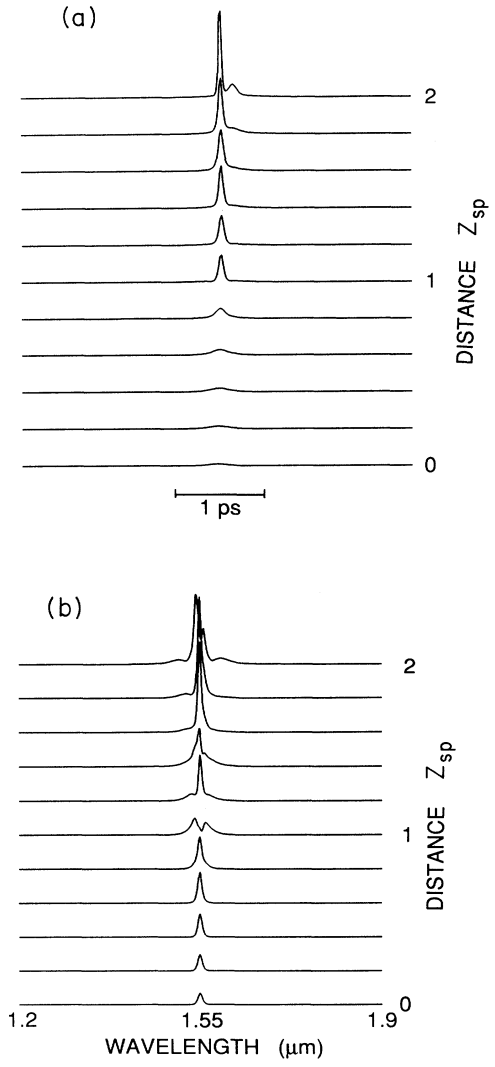

FIG. 16. A NLS soliton noncoherently interacting with erbium ions. (a) Wave form, (b) spectrum. A clear evolution from an $N=1$ to $N=2$ soliton is observed. $T_2=100$ fs, $\tau_s=250$ fs, and there is no SSFS. Wave-form distortion at $Z=2Z_{sp}$ is due to the pulse narrowing that reduces the pulse width to less than T_2, resulting in a coherent interaction.

shorter than T_2. This results in bigger changes in both M and F as shown in Eqs. (8.5) and (8.6). Hence a coherent interaction is initiated eventually. The evidence for this is seen in the asymmetric wave-form distortion on the right-hand side of the NLS wave form at $Z=2Z_{sp}$. The amplification of the NLS soliton shown in Fig. 15(a) is rather more complicated than that in Fig. 16, indicating that the NLS is coherently interacting with the erbium ions in Fig. 15(a). It should be noted that a coherent interaction, which generates multiple short pulses, occurs although the amplitude of the input soliton pulse is much lower than that of $\pi-2\pi$ pulses.

IX. CONCLUSION

The coexistence of the SIT-NLS soliton has been examined. A condition for the mixed soliton state is

$$|k''_{\text{SIT-NLS}}|=\frac{n_2h^2}{2\pi\lambda|p_{21}|^2} .$$

A simple derivation of the equality has been also presented by equating $P_{\text{SIT}}=P_{N=1(\text{NLS})}$ for a given input soliton pulse width. It is concluded mathematically that the SIT-NLS soliton exists, but it seems to be difficult to realize it in actual silica-based erbium-doped fibers, since the peak intensity of a 2π pulse is much larger than that of a conventional $N=1$ NLS soliton pulse. In other words, n_2 should be much smaller or $|D|$ should be much larger. It is important to note that the phase change in the SIT-NLS soliton is governed by the NLS component and the pulse delay due to the resonance is determined only by the SIT component when the detuning is zero.

The conditions for observing a pure SIT soliton in a silica-based optical fiber were also presented, in which it has been shown that the utilization of input pulse widths of a few hundred picoseconds to nanoseconds will be practical, by cooling the fiber to less than 10 K. In such cases the pulse delay due to the SIT is of the order of ns. Finally, the SIT-NLS solitons were computer-run and it is confirmed that a stable 2π SIT-$N=1$ NLS soliton exists. However, high-order SIT-NLS solitons always split into multiple $2\pi/N=1$ SIT-NLS soliton pulses. It should be noted that the NLS property can be preserved when $Z_{sp}\ll L_{abs}$.

NLS solitons which coherently or noncoherently interact with erbium ions are described. When the NLS soliton interacts with the erbium ions, coherent pulsation that produces multiple pulses is obtained. It should be noted that a coherent interaction occurs although the amplitude of the input soliton pulse is much lower than that of $\pi-2\pi$ pulses.

ACKNOWLEDGMENTS

The authors would like to express their sincere thanks to Professor H. A. Haus for stimulating discussions and comments. Thanks are also due to Professor E. P. Ippen for discussion on the SIT and photon echo and to Dr. S. Shimada and Dr. H. Ishio for their encouragement.

APPENDIX

By putting $y=\tau-\gamma\zeta$ and $u=\frac{1}{2}\mathcal{E}=2\beta\,\text{sech}2\beta y$, (2.5) and (2.6) are rewritten as

$$\frac{\partial v_1}{\partial y}-uv_2=-i\xi v_1 , \tag{A1}$$

$$\frac{\partial v_2}{\partial y}+u^*v_1=i\xi v_2 . \tag{A2}$$

Thus, we obtain an equation for v_1

$$\frac{d^2v_1}{dy^2}-\left[\frac{1}{u}\frac{du}{dy}\right]\frac{dv_1}{dy}+\left[-i\xi\frac{1}{u}\frac{du}{dy}+|u|^2+\xi^2\right]v_1=0 . \tag{A3}$$

When we put

$$v_1=C\,\text{sech}2\beta y e^{i\xi y} , \tag{A4}$$

v_1 satisfies (A3). Using (A4), v_2 is calculated as

$$\begin{aligned} v_2&=\frac{1}{u}\left[\frac{dv_1}{dy}+i\xi v_1\right] \\ &=-\frac{C}{\cos\phi}\sinh(2\beta y+i\phi)\,\text{sech}2\beta y e^{i\xi y} , \end{aligned} \tag{A5}$$

where

$$\tan\phi=-\xi/\beta .$$

Thus, one obtains

$$\begin{aligned} |v_1|^2+|v_2|^2&=C^2[\text{sech}^2 2\beta y+(-\tanh 2\beta y+i\xi/\beta) \\ &\quad\times(-\tanh 2\beta y-i\xi/\beta)] \\ &=C^2[1+(\xi/\beta)^2]=\frac{C^2}{\cos^2\phi} . \end{aligned} \tag{A6}$$

In a two-level system, $|v_1|^2+|v_2|^2=1$, so that

$$C=\pm\cos\phi . \tag{A7}$$

Taking $C=-\cos\phi$, we obtain

$$v_1=-\cos\phi\,\text{sech}2\beta(\tau-\gamma\zeta)e^{i\xi(\tau-\gamma\zeta)} , \tag{A8}$$

$$\begin{aligned} v_2&=\sinh[2\beta(\tau-\gamma\zeta)+i\phi]\,\text{sech}2\beta(\tau-\gamma\zeta) \\ &\quad\times e^{i\xi(\tau-\gamma\zeta)} . \end{aligned} \tag{A9}$$

For reference in the case of an $N=1$ NLS soliton, v_1 and v_2 or $u(y,0)=2\eta\,\text{sech}(2\eta y)e^{-i2\xi y}$, which pertains to the pole $\zeta\,(=\xi+i\eta)$, are given by [26]

$$v_1=\frac{1}{2\sqrt{i}}\text{sech}(2\eta y)e^{-(\eta+i\xi)y} , \tag{A10}$$

$$v_2=\frac{\sqrt{i}}{2}\text{sech}(2\eta y)e^{(\eta+i\xi)y} . \tag{A11}$$

*Electronic address: nakazawa%lightwave.ntt.jp.

[1] R. J. Mears, L. Reekie, I. M. Jauncy, and D. N. Payne, Electron. Lett. **23**, 1026 (1978).
[2] E. Desurvire, J. R. Simpson, and P. C. Becker, Opt. Lett. **12**, 888 (1987).
[3] Y. Kimura, K. Suzuki, and M. Nakazawa, Electron. Lett. **25**, 1656 (1989).
[4] B. J. Ainslie, K. J. Blow, A. S. Gouveia-Neto, P. G. J. Wigley, A. S. B. Sombra, and J. R. Taylor, Electron. Lett. **26**, 186 (1990).
[5] I. Yu. Khrushchëv, A. B. Grudinin, E. M. Dianov, D. V. Korobkin, Jr., V. A. Semenov, and A. M. Prokhorov, Electron. Lett. **26**, 457 (1990).
[6] V. V. Afanasjev, E. M. Dianov, A. M. Prokhorov, and V. N. Serkin, Sov. Tech. Phys. Lett. (to be published).
[7] M. Nakazawa, K. Kurokawa, H. Kubota, K. Suzuki, and Y. Kimura, Appl. Phys. Lett. **57**, 653 (1990).
[8] M. Nakazawa, K. Kurokawa, H. Kubota, and E. Yamada, Phys. Rev. Lett. **65**, 1881 (1990).
[9] S. L. MaCall and E. L. Hahn, Phys. Rev. Lett. **18**, 908 (1967); Phys. Rev. **183**, 457 (1969).
[10] C. K. N. Patel and R. E. Slusher, Phys. Rev. Lett. **19**, 1019 (1967).
[11] H. M. Gibbs and R. E. Slusher, Phys. Rev. Lett. **24**, 638 (1970).
[12] G. L. Lamb, Jr., Rev. Mod. Phys. **43**, 99 (1971).
[13] J. Hegarty, M. M. Broer, B. Golding, J. R. Simpson, and J. B. MacChesney, Phys. Rev. Lett **51**, 2033 (1983).
[14] M. M. Broer and B. Golding, J. Opt. Soc. Am. B **3**, 523 (1986).
[15] A. Hasegawa and F. Tappert, Appl. Phys. Lett. **23**, 142 (1973).
[16] A. Guzman, M. Romagnoli, and S. Wabnitz, Appl. Phys. Lett. **56**, 614 (1990).
[17] A. I. Maimistov and E. A. Manykin, Zh. Eksp. Teor. Fiz. **85**, 1177 (1983) [Sov. Phys.—JETP **58**, 685 (1983)].
[18] I. V. Mel'nikov, R. F. Nabiev, and A. V. Nazarkin, Opt. Lett. **15**, 1348 (1990).
[19] H. A. Haus, Rev. Mod. Phys. **51**, 331 (1979).
[20] V. E. Zakharov and A. B. Shabat, Zh. Eksp. Teor. Fiz. **61**, 118 (1971) [Sov. Phys.—JETP **34**, 62 (1972)].
[21] E. Desurvire and J. R. Simpson, J. Lightwave Technol. **7**, 835 (1989).
[22] G. P. Agrawal and M. J. Potasek, Phys. Rev. A **33**, 1765 (1986).
[23] W. H. Press, B. P. Flannery, S. A. Teukolsky, and W. T. Vetterling, *Numerical Recipes, The Art of Scientific Computing* (Cambridge University Press, Cambridge, England, 1986).
[24] J. P. Gordon, Opt. Lett. **11**, 662 (1986); see also F. M. Mitschke and L. F. Mollenauer, Opt. Lett. **11**, 659 (1986).
[25] H. A. Haus and M. Nakazawa, J. Opt. Soc. Am. B **4**, 381 (1987).
[26] J. Satsuma and N. Yajima, Suppl. Prog. Theor. Phys. **55**, 284 (1974).